

# HYBRID MONTE CARLO/ DETERMINISTIC METHODS FOR ACCELERATING ACTIVE INTERROGATION MODELING

DOUGLAS E. PELOW,\* THOMAS M. MILLER, BRUCE W. PATTON,  
and JOHN C. WAGNER

Oak Ridge National Laboratory, Reactor and Nuclear Systems Division  
P.O. Box 2008, Oak Ridge, Tennessee 37831-6172

Received February 29, 2012

Accepted for Publication April 9, 2012

*The potential for smuggling special nuclear material (SNM) into the United States is a major concern to homeland security, so federal agencies are investigating a variety of preventive measures, including detection and interdiction of SNM during transport. One approach for SNM detection, called active interrogation, uses a radiation source, such as a beam of neutrons or photons, to scan cargo containers and detect the products of induced fissions. In realistic cargo transport scenarios, the process of inducing and detecting fissions in SNM is difficult due to the presence of various and potentially thick materials between the radiation source and the SNM and the practical limitations on radiation source strength and detection capabilities. Therefore, computer simulations are being used, along with experimental measurements, in efforts to design effective active interrogation detection systems. The computer simulations primarily consist of simulating radiation transport from the source to the*

*detector region(s). Although the Monte Carlo method is predominantly used for these simulations, difficulties persist related to calculating statistically meaningful detector responses in practical computing times, thereby limiting their usefulness for design and evaluation of practical active interrogation systems. In previous work, the benefits of hybrid methods that use the results of approximate deterministic transport calculations to accelerate high-fidelity Monte Carlo simulations have been demonstrated for source-detector-type problems. In this work, hybrid methods are applied and evaluated for three example active interrogation problems. Additionally, a new approach is presented that uses multiple goal-based importance functions depending on a particle's relevance to the ultimate goal of the simulation. Results from the examples demonstrate that the application of hybrid methods to active interrogation simulations dramatically increases their calculational efficiency.*

## I. INTRODUCTION

The U.S. Department of Homeland Security (DHS) has a goal of scanning cargo containers entering the United States for illicit nuclear material. The goal addresses shipments by land, sea, and air. One method under study by the U.S. Department of Energy and other federal agencies for detecting fissionable material is active interrogation—a system that uses a radiation source, such as a collimated beam of neutrons or photons, to scan

cargo containers and detect the products of induced fissions from any fissionable material.

### I.A. Active Interrogation

Active interrogation involves directing radiation (e.g., neutrons and/or photons) into a cargo container (e.g., luggage, a 55-gal drum, a Sea-Land container, or the cargo hold of a large boat or airplane) suspected of carrying special nuclear material (SNM) and then detecting the products of any subsequent fission reactions. This approach differs from passive detection, which relies on

\*E-mail: pepelowde@ornl.gov

detecting the natural radiation emitted from SNM. Several active interrogation techniques under evaluation attempt to observe different combinations of interrogating radiation sources, detector types, and fission reaction effects. Detecting fissionable material is conceptually straightforward, but thick and diverse materials between the fissionable material and the interrogation source act as shielding for both the interrogating radiation and the resulting fission radiation, thus complicating the task. When using isotropic sources with large standoff distances  $R$ , one has to contend with  $1/R^2$  geometric attenuation of the active interrogation beam particles. If the detectors have similar standoff distances, then the detection of fission radiation also suffers from another  $1/R^2$  geometric attenuation. SNM could easily be encased in an engineered shield specifically constructed to reduce fission signatures. This would cause very few fission events to be detected and therefore would require a very intense interrogating source strength.

Aside from the basic physics, active interrogation scanning systems for cargo vessels and shipping containers are also subject to real-world engineering limitations. These constraints include maximum allowable dose to operations personnel, maximum allowable dose to cargo materials, low induced radioactivity (activation) of the cargo, limit on scan time to preserve cargo throughput rate, low false-negative rate, low false-positive rate, reasonable system installation costs, and reasonable maintenance and operations costs. Large source strengths, which help increase the number of events seen by the detectors, are limited not only by the dose rate requirements but also by electrical power needs and heat removal requirements. Detectors and their analysis electronics can range from simple to exotic,<sup>1,2</sup> drastically affecting cost and reliability. For an active interrogation system to be successful in realistic cargo transport scenarios, it will have to utilize a mix of source particles that can penetrate different materials.

The challenge is to find the right combination of source parameters, fission signature emissions, and detection schemes that can detect the threat object (uranium, plutonium, or other SNM) in cargo containers of various sizes with a wide variety of cargo materials. Active interrogation sources are generally characterized by particle type (neutron, gamma, muon, etc.), energy dependency (monoenergetic or polyenergetic), production source (accelerators or natural decay), and operational mode (pulsed or steady state). The fission signatures typically of interest are prompt or delayed neutrons or gamma rays, or even induced multiplication. Detection schemes include count rate or energy spectrum, steady state or timed with the source, coincidence measurements, differential die-away, and many others. Cargo materials range from water-based agricultural products, which are difficult for neutrons to penetrate, to heavy industrial equipment made of metal, which is difficult for photons to penetrate. As an example, consider active interrogation

using photons to produce photonuclear effects in the fissile material. Hydrogenous cargo would allow the high-energy photons to penetrate rather easily, while outgoing neutrons from fission events would attenuate rapidly. In contrast, a cargo mixture with a high metal content would attenuate the incoming photons while offering less attenuation to outgoing neutrons. The large number of source and cargo combinations severely limits the practicality of using laboratory experiments to compare different interrogation strategies. The use of simulations can narrow the range of applicability of various concepts followed by laboratory experiments to provide maximum information and confirm detection capabilities.

### I.B. Simulation of Active Interrogation

Computer simulation is required to explore the effectiveness of the various radiation source and detector options for active interrogation. The Monte Carlo method, which samples the probabilities of nuclear radiation to scatter and penetrate material, is used to determine (a) the transmission of source radiation through the cargo materials, (b) the amount of fission in the SNM, (c) the radiation released from the fission, (d) the mode of radiation transport from the container, and (e) the radiation interaction with the detectors. Everything that makes active interrogation a difficult problem in the real world also makes it difficult for computer simulation—only a small fraction of the simulated source particles reaches the SNM to cause fission, and only a small fraction of the fission signature radiation reaches the detectors. Similar to detector counting statistics, every Monte Carlo result has some stochastic variance. Calculations, even for simple models of systems, may require long computation times or many processors to reduce statistical uncertainty of the final results to acceptable levels.<sup>3</sup> The calculations described in Ref. 3 took 1 to 6 h on 30 processors, depending on the materials inside the shipping container. To evaluate the detection systems, Monte Carlo calculations must be done in pairs—with and without the threat object—so that the signal from the threat object can be seen as a difference from the background signal coming from the rest of the container. If Monte Carlo simulations of active interrogation systems could be performed hundreds of times faster, dramatic improvements in design would be realized and optimization studies using more-detailed models could be completed.

This paper describes work in applying automated variance reduction using hybrid deterministic/Monte Carlo methods to active interrogation problems. The MAVRIC sequence,<sup>4</sup> part of the SCALE package<sup>5a</sup> of codes used for criticality, shielding, and reactor analysis, uses a coarse-mesh discrete ordinates calculation to determine the

<sup>a</sup>Reference 5 is also available from the Radiation Safety Information Computational Center at Oak Ridge National Laboratory (ORNL) as CCC-750.

space- and energy-dependent importance parameters for a detailed Monte Carlo simulation. The CADIS (Consistent Adjoint-Driven Importance Sampling) method<sup>6,7</sup> is used to compute both the target weight windows and a consistent biased source, both functions of space and energy. The MAVRIC sequence is automated—handling the calculations for the variance reduction parameters with only minor additional input from the user—and highly capable in terms of accelerating traditional source-detector problems.

Most applications to which the MAVRIC sequence has been successfully applied have been source-detector problems that bias source particles such that particles moving toward the detector with energies that will contribute to the detector response are simulated more often than those moving away from the detector or those with inconsequential energies. Active interrogation problems differ from typical source-detector problems in that source particles must travel from the source to the fissionable material and cause fission, and then secondary particles must travel to a detector. The importance of particles contributing to the detector(s) is no longer dependent on only space and energy but is also dependent on the path and particles of interest (i.e., incoming active interrogation source particles or outgoing particles produced from the active interrogation source particles’ interactions with other materials).

Storing two importance maps in memory at the same time could be impractical for large problems. Setting a trigger to select each particle map is not as straightforward as setting an interaction flag or using a particle time. Doing the latter may start the biasing of particles toward the detector too early, not allowing for deeper penetration into, or completion of fission chains within, the threat object. The approach used in this study is to break the problem into separate steps (source to threat object and threat object to detector) and fully develop biasing parameters for each step.

## II. THEORY

### II.A. CADIS Review

Wagner and Haghghat<sup>6,7</sup> developed and fully described CADIS, so only a brief review is given here. The goal of the Monte Carlo calculation is to compute the flux from a unit source  $\psi(\vec{r}, E)$  over some detector region and then compute the response  $R$ , using a response function  $\sigma(\vec{r}, E)$ , to determine total reaction rate, dose, etc.:

$$R = \iint \sigma(\vec{r}, E)\psi(\vec{r}, E) dE dV . \quad (1)$$

In a Monte Carlo simulation, particles are sampled from the source distribution  $q(\vec{r}, E)$ , followed through the ge-

ometry, and tallied with the response function in the appropriate portion of phase space. Equivalently, the response can also be found from integrating the source with the adjoint flux  $\psi^+(\vec{r}, E)$ :

$$R = \int q(\vec{r}, E)\psi^+(\vec{r}, E) dE dV , \quad (2)$$

where the adjoint calculation uses the adjoint source of  $q^+(\vec{r}, E) = \sigma(\vec{r}, E)$ . To minimize the variance in the Monte Carlo calculation of  $R$ , Wagner and Haghghat showed that the biased source distribution,

$$\hat{q}(\vec{r}, E) = \frac{1}{R} q(\vec{r}, E)\psi^+(\vec{r}, E) , \quad (3)$$

could be used. Particles sampled from the biased distribution are born with a weight of  $w_0 \equiv q/\hat{q}$ . A set of weight window target values  $\bar{w}(\vec{r}, E)$  can be constructed to match these birth weights by using

$$\bar{w}(\vec{r}, E) = \frac{R}{\psi^+(\vec{r}, E)} . \quad (4)$$

If the adjoint is known precisely, then these weight window target values and the biased source should yield a zero-variance estimate of  $R$ . A good estimate of the adjoint should significantly reduce the variance in calculating  $R$ .

CADIS is implemented by first estimating the adjoint flux  $\psi^+(\vec{r}, E)$ , integrating the adjoint flux and true source distribution to estimate  $R$ , and then forming the biased source distribution and weight window targets for use in the Monte Carlo calculation. Note that this formulation of the weight window target values makes the importance map “consistent” with the biased source; a source particle is born with an initial weight matching the target weight value of the location and energy where it is born.

CADIS has been implemented into two code systems at ORNL: the ADVANTG code system<sup>8</sup> for MCNP and the MAVRIC sequence<sup>4</sup> of SCALE, both of which use the adjoint scalar fluxes produced by the Denovo discrete ordinates ( $S_N$ ) code.<sup>9</sup> The resulting importance map is a function of only space and energy, and the source is biased only in space and energy. Recent work at ORNL has investigated extending the above formalism to also include particle direction.<sup>10</sup>

Both ADVANTG and MAVRIC were developed to be as automatic as possible. The user creates the same input file as for an analog Monte Carlo calculation and then provides a small amount of additional information for the discrete ordinates adjoint calculation using Denovo. This additional information consists of the spatial mesh and the adjoint source spatial and energy distributions, which should correspond to the tally that the user wishes to optimize. Default parameters for the Denovo calculation, such as quadrature order, Legendre order, upscatter capability, etc., can also be overridden by the

user. ADVANTG and MAVRIC then use the information to construct a voxelized version of the geometry and adjoint source, relieving the user of the task of preparing multiple models for the deterministic and Monte Carlo codes.

**II.B. Forward-Weighted CADIS Review**

The CADIS method described above is a very efficient hybrid method for computing a single tally. For applications that require the calculation of many tallies, applying the CADIS method one tally at a time could be difficult and time-consuming. This would be even more challenging for a large mesh tally.

One way to compute multiple tallies at once with CADIS is to simply include an adjoint source in the adjoint calculation for each tally in the Monte Carlo problem. Unfortunately, when multiple adjoint sources (tallies) are used with the CADIS methodology, Monte Carlo particles tend to be transported only to the tally that is closest to the true source and not to the other tallies. Increasing the adjoint source strength corresponding to the tallies farther away from the true source tends to improve the relative uncertainties of those tallies. To compute all of the tallies of the problem with about the same relative uncertainty, it has been determined that the adjoint source strength in the deterministic adjoint calculation should be inversely proportional to the expected Monte Carlo response of those tallies.

This leads to a natural extension of the CADIS method, where the adjoint source is inversely weighted by the forward estimate of the tally responses: forward-weighted CADIS (FW-CADIS) (Refs. 11, 12, and 13). First, a forward  $S_N$  calculation is performed to estimate the expected tally results. Next, an adjoint  $S_N$  calculation is performed, for which the adjoint source is inversely weighted by the expected tally estimates from the forward  $S_N$  calculation, to obtain the space- and energy-dependent adjoint importance function. Then, the standard CADIS approach is used—an importance map (target weight windows) and a biased source are calculated using the adjoint flux computed from the adjoint  $S_N$  calculation.

For example, if the goal is to calculate a detector response function  $\sigma_d(E)$ , such as dose rate using flux-to-dose-rate conversion factors, over a volume [defined by  $g(\vec{r})$ ] corresponding to the mesh tally, then instead of simply using  $q^+(\vec{r}, E) = \sigma_d(E)g(\vec{r})$ , the adjoint source would be

$$q_i^+(\vec{r}, E) = \frac{\sigma_d(E)g(\vec{r})}{\int \sigma_d(E)\phi(\vec{r}, E) dE} , \tag{5}$$

where  $\phi(\vec{r}, E)$  is the  $S_N$  estimate of the forward flux and the energy integral is over the voxel at position  $\vec{r}$ . The adjoint source is nonzero only where the mesh tally is

defined [ $g(\vec{r})$ ], and its strength is inversely proportional to the forward estimate of dose rate for that voxel.

In MAVRIC, there are two options for forward weighting. For tallies over some area where the entire group-wise flux is needed with low relative uncertainties, the adjoint source is weighted inversely by the forward flux estimate,  $\phi(\vec{r}, E)$ . The other option is for a tally where only an energy-integrated quantity is desired. In this case the adjoint source is inversely weighted by that energy-integrated quantity,  $\int \sigma_d(E)\phi(\vec{r}, E) dE$ . For a tally where the total flux is desired, the response in the adjoint source is  $\sigma_d(E) = 1$ .

**II.C. Hybrid Methods Applied to Active Interrogation Problems**

Positive detection of a threat object depends on determining small differences in the detector response between configurations with and without the threat object. The particles coming from the threat object to the detector provide the desired signal, which can be small compared to all of the particles arriving at the detector that were induced by the interrogation source through reactions with the rest of the materials (called “active background”). In simulations, the incoming source particles can be biased to enhance interaction with the threat object, or the outgoing particles produced in the threat object can be biased to enhance detector response, but present simulation capabilities do not easily handle the simultaneous occurrence of both biases in a general manner [MCNP (Ref. 14) can use different importance maps for different particle types; MCNPX (Ref. 15) can use multiple importance maps based on time]. Hence, to deal effectively with the difficult problem of simulating an active interrogation system, the problem can be divided into several steps, and hybrid methods can be applied to each step. In the first step, particles are transported from the interrogation source to the threat object to generate the sources for the second step. The particles that result from interactions in the threat object become the source for the next step and need to be characterized well in terms of their spatial and energy distributions. For determining the fission rate in a small volume of SNM, the CADIS method can be used to significantly improve the calculational efficiency. For determining the active background produced by the interrogation source over a large volume of surrounding materials, a calculation using the FW-CADIS method can be performed to obtain more uniform relative uncertainties over the large volume.

For the second step, the detector response needs to be determined for the various sources of induced particles. For typical detectors, which are small compared with the overall problem, a multiple-source calculation using the CADIS method is sufficient. Detectors that are large compared to the size of the problem may require use of the FW-CADIS method. For some problems, more than two steps may be required to model particles produced

in surrounding materials that lead to fission in the threat object. For example, a high-energy photon interrogation source could induce photonuclear reactions in surrounding materials, which could then cause fission in the threat object. This large-volume-induced photo-neutron source could be determined using an FW-CADIS approach and added to the interrogation source when determining the interaction rate within the threat object.

A separate calculation also must be performed without the threat object present to determine the detector response due solely to source particles interacting with surrounding material. Variance reduction can be applied to this calculation as well.

### III. EXAMPLE PROBLEMS

In Secs. III.A, III.B, and III.C, the hybrid methods described in Sec. II are applied to three relevant active interrogation problem configurations of increasing size and complexity.

#### III.A. Barrel-Scanning System

A simple example of an active interrogation system for scanning 55-gal drums is shown in Fig. 1, which illustrates a system similar to those discussed in Refs. 16 and 17. A 14.1-MeV,  $10^9$  n/s isotropic source (S) and a polyethylene-moderated  $^3\text{He}$  detector are positioned on opposite sides of a 55-gal barrel. The goal is to compute the difference in detector signal between two water-filled

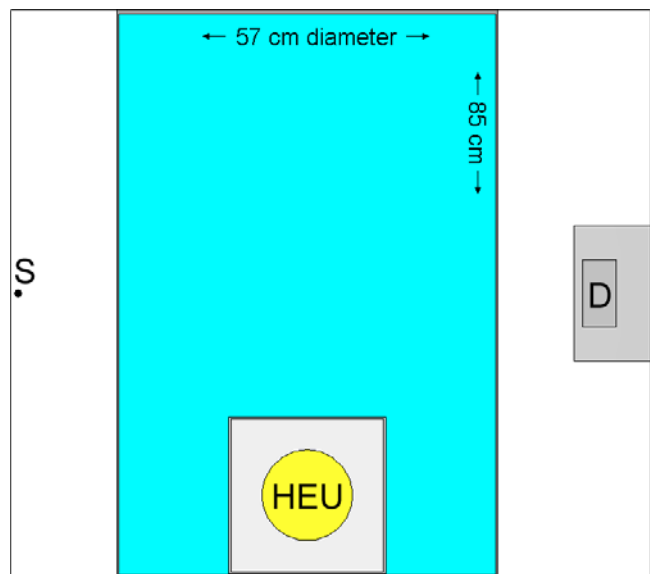


Fig. 1. Geometry for a barrel-scanning system. The 25 kg of HEU sits at the bottom of the barrel in a balsa box. The source (S) is on the left, and the detector (D) is on the right.

barrels, with and without a spherical threat object (radius = 6.83 cm) containing 25 kg of highly enriched uranium (HEU) (an International Atomic Energy Agency significant quantity<sup>18</sup>) in a balsa box (to avoid criticality). A single calculation is performed for the barrel containing only water, and a two-step calculation is performed for the barrel containing HEU. Note that all calculations for this problem considered neutrons only.

For the barrel without the HEU threat object, a MAVRIC calculation that was optimized to transport particles to the detector was performed using a coarse-mesh importance map ( $19 \times 26 \times 26$  and 27 groups) and a final Monte Carlo calculation using a 200-group cross-section library. The  $^3\text{He}(n, p)^3\text{H}$  interaction rate in the detector was calculated to be  $6.43 \times 10^3$  interactions/s  $\pm 0.4\%$ . This calculation took 1 h on a single processor to complete.

For the barrel with the HEU, the fission rate of the HEU was first calculated. This calculation was done using the CADIS method to optimize neutron transport to the HEU, so the importance map ( $28 \times 37 \times 36$ ) used more detail near the source and the HEU and little detail near the detector. In 1 h of computing time, the total fission neutron production rate in the HEU was calculated to be  $4.16 \times 10^7$  n/s  $\pm 0.7\%$ . The fission neutron production rate mesh tally is shown in Fig. 2. Note that the highest fission rates appeared on the outer edge of the sphere, in the quadrant facing the source.

The second step of the calculation with HEU in the barrel used both the interrogation source and the HEU fission source (with multiplication turned off so as to not double count fission neutrons in the HEU). This calculation used CADIS to more effectively transport neutrons to the detector with an importance map of  $28 \times 42 \times 40$ , which included planes to provide more detail in the threat object and the detector. The total detector interaction rate for the barrel containing HEU was calculated to be  $7.74 \times 10^3$  interactions/s  $\pm 0.5\%$ , which is 20% higher than the detector response without the threat object. This calculation also took 1 h. Note that the mesh

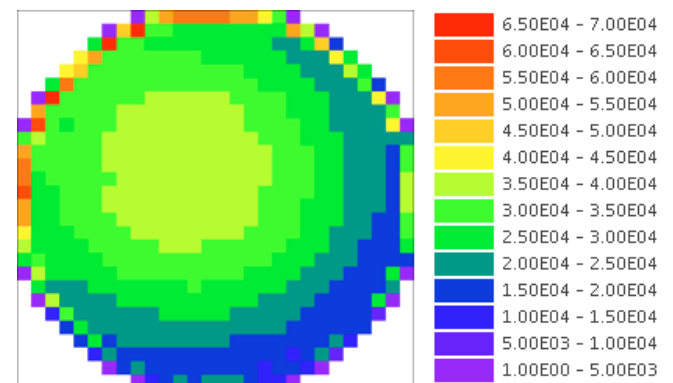


Fig. 2. Fission distribution in the HEU sphere, shown for the same slice as shown in Fig. 1.

source used in this step contained uncertainties in the strength of each voxel, which are not accounted for in the uncertainty estimates of the final tally. Tests using 30 different versions of the mesh source (replicants made with different starting random numbers in step 1) and 30 replicants of step 2 with the same mesh source showed that the uncertainty in the mesh source contributed very little to the uncertainty of the final detector interaction rate. Nearly all of the uncertainty in the detector interaction rate was from source sampling and particle transport in step 2.

To obtain the same level of statistical uncertainty (~0.5%) with analog calculations, it would take an estimated 270 h for the water-only barrel and 390 h for the barrel with the threat object. Use of the automated hybrid methods for these simulations provides a substantial savings in calculation time.

### III.B. Single Shipping Container

For a larger problem, consider a system used to scan 12-m (40-ft) long Sea-Land cargo containers using a <sup>2</sup>H-<sup>2</sup>H source on one side and three types of detectors on the other. For this demonstration, the container was modeled as a homogenous mixture representing a specific cargo type inside a thin steel shell, which is similar to the system evaluated in Ref. 3. Three different mixtures filling the container were investigated.<sup>19</sup> These are listed in Table I. The container was modeled 1 m above a concrete slab, as shown in Fig. 3. Simulations were made for containers with and without a 25-kg HEU spherical threat object in the center of the cargo container. Note that 25 kg of HEU in any of these materials will not be critical, having *k<sub>eff</sub>* values of about 0.85.

The <sup>2</sup>H-<sup>2</sup>H source was modeled as a point isotropic source of 2.45-MeV neutrons located 28.08 cm (~11 in.) from the side of the container. Neutrons can create gamma rays in the cargo material through scattering and absorp-

TABLE I  
Materials Used for the Homogenous Shipping Container Model\*

Material/Constituents by Weight Fraction	Density (g/cm <sup>3</sup> )
PNNL <sup>a</sup> hydrogenous cargo Water	0.2
DHS iron/organic mixed cargo 50% Fe, 23.5% O, 23.5% C, 3% H	0.4
PNNL high-iron mixed cargo 60% Fe, 19% C, 10% Al, 4% O, 3.99% N, 3% H, 0.01% Cl	0.6

\*Reference 19.

<sup>a</sup>PNNL = Pacific Northwest National Laboratory.

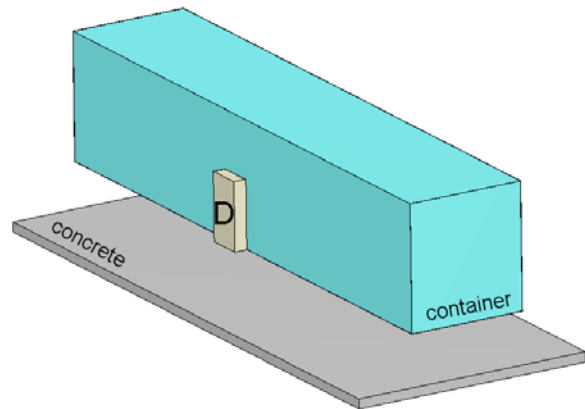


Fig. 3. Homogenous cargo container above a concrete slab with the detector bank (D) visible. (The source is behind the container.)

tion interactions. When the threat object is present, fissions producing both neutrons and gamma rays can occur.

The bank of detectors, shown in Fig. 4, includes a large cylindrical sodium iodide (NaI) photon detector, a small high-purity germanium (HPGe) photon detector, and five cylindrical <sup>3</sup>He neutron detectors surrounded by polyethylene. The goal is to determine the change in the detector count rates due to the presence of the HEU sphere.

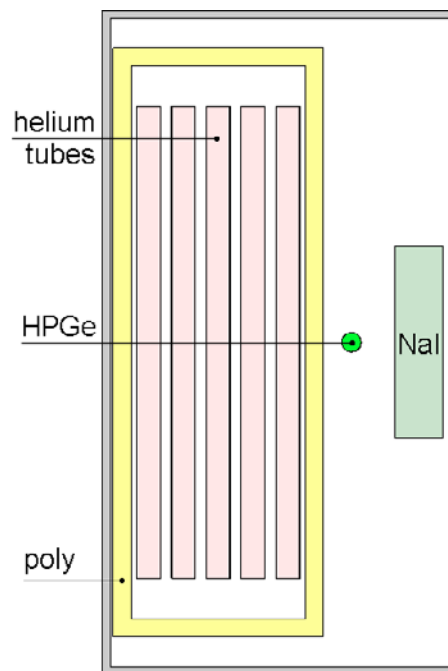


Fig. 4. Detectors inside the detector bank (left to right) include five <sup>3</sup>He tubes surrounded by polyethylene, a small HPGe detector, and a large NaI detector. The detector bank is 74.81 cm wide and 140.31 cm high.

Note that any neutrons detected with energies >2.45 MeV must have originated from fission.

The calculations for each combination of cargo type and detector without the uranium threat object required one MAVRIC calculation and used the CADIS method for acceleration. The adjoint source was the appropriate detector response function for the total count rate located in the appropriate detector volume. For the neutron detector, the importance map included only neutrons. For the gamma ray detectors, a coupled neutron-gamma importance map was used.

The calculations for models with the 25-kg HEU sphere required two steps. First, the fission density was tallied on a small grid overlaying the sphere. For this MAVRIC calculation, the adjoint source was the fission cross section, and only a neutron importance map was created. The second MAVRIC simulation, with multiplication turned off, used the original <sup>2</sup>H-<sup>2</sup>H source and the fission mesh source (with fission photons added). The adjoint source for this step was the appropriate detector response function for the total count rate located in the appropriate detector volume. Note that this is the same adjoint  $S_N$  calculation as the “no threat object” case above.

A total of nine sets of calculations were performed—for each combination of the three different cargo materials and three different detectors. Within each set, six MAVRIC calculations were performed—the first two were performed only to provide analog results for comparison purposes:

1. analog calculation without the HEU
2. analog calculation with the HEU
3. calculation using CADIS of the detector response due to the active interrogation source without the HEU
4. calculation using CADIS with the threat object to determine the fission rate in the HEU (step 1)

5. calculation using CADIS to determine the detector response due to both the active interrogation source and the fission particles from the HEU (step 2)
6. calculation using CADIS to determine the detector response due to only the fission particles from the HEU.

Calculations 1 and 3 should obtain the same result for the container without the HEU, with the CADIS calculation being faster. The two-step approach using calculations 4 and 5 should match the analog result from calculation 2. The effect of the HEU is the difference between the corresponding with/without calculations (calculations 1/2 and calculations 3/5). In this case, that difference is too small to be seen compared to the statistical uncertainties in calculations 3 and 5; therefore, calculation 6 was used to compute the detector response to only the fissions in the HEU.

As an example of the nine sets of calculations, the results for the medium-density DHS iron/organic material and the HPGe detector are shown in Table II. Each of the analog calculations was run for 24 h and yielded detector count rates with 4.5% to 5.0% relative uncertainties. The difference between the with-HEU and without-HEU results is  $1.09 \times 10^4$  reactions/s·Ci<sup>-1</sup> ± 60%. It would take a very long time to converge each calculation sufficiently to obtain a difference with a reasonably low uncertainty.

The CADIS calculation without the HEU was run for 12 h and gave the same result (within about 1σ) as the 24-h analog calculation but with a much lower relative uncertainty (calculation 3 in Table II). Target weight windows from the importance map are shown in Fig. 5 for source neutrons to get to the fissile threat object (step 1) and in Fig. 6 for photons to get to the HPGe detector. The figure of merit (FOM) for the CADIS calculation, including the  $S_N$  time, was about 32 times higher than that

TABLE II

Results for the Set of Calculations for the DHS Iron/Organic Mixed Cargo\* and the HPGe Neutron Detector

Calculation	Time (min)		Count Rate (Reactions/s·Ci <sup>-1</sup> )	Relative Uncertainty (%)	Monte Carlo FOM (min <sup>-1</sup> )
	Denovo $S_N$	Monte Carlo			
1. Analog without HEU		1442	9.365E+04 <sup>a</sup>	4.9	0.287
2. Analog with HEU		1443	1.046E+05	4.5	0.348
3. CADIS without HEU	70	643	9.901E+04	1.2	10.1
4. CADIS fission rate (step 1)	83	62	7.292E+07	0.4	1210.0
5. CADIS (step 2)	104	465	9.963E+04	1.4	10.9
6. CADIS fission only	105	462	3.166E+03	1.0	22.4

\*DHS iron/organic mixed cargo density is 0.4 g/cm<sup>3</sup>.

<sup>a</sup>Read as  $9.365 \times 10^4$ .

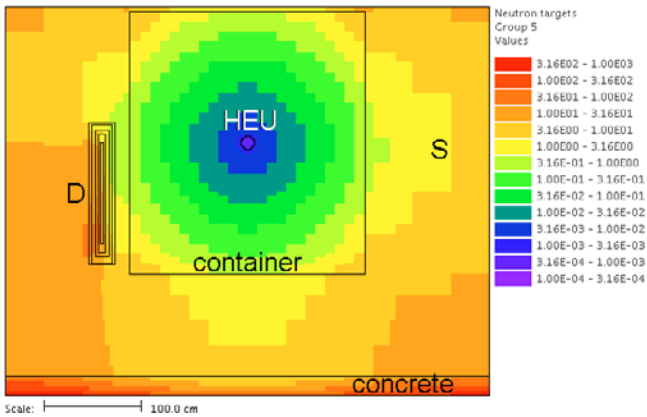


Fig. 5. Importance map weight window target values for 1-MeV neutrons for step 1: determination of the fission rate in the HEU.

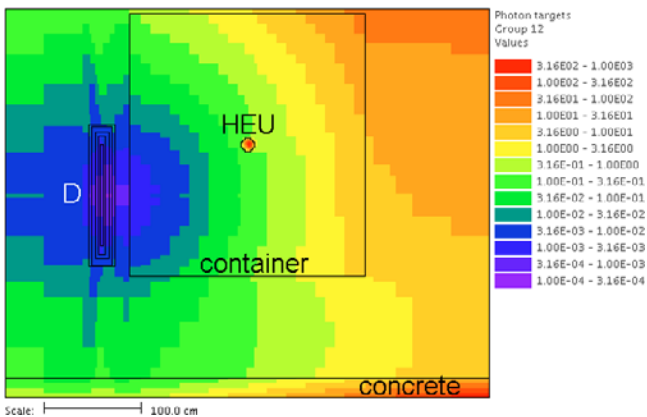


Fig. 6. Importance map weight window target values for 1-MeV photons for step 2: determination of the HPGe detector response.

for the analog calculation. For the two-step CADIS calculations for the cargo container with the HEU, ~2.5 h was required to compute the fission source and ~9.5 h was required to compute the detector response. The result of the two-step calculation was the same as the analog calculation (within about 1σ) but had a much lower relative uncertainty. Including the  $S_N$  and Monte Carlo times of both steps, the FOM of the two-step CADIS method is 20 times higher than that of the analog.

Even though both the with-HEU and the without-HEU CADIS results converged better than the analog results, the difference between the two results also suffers from a very large uncertainty ( $623 \text{ reactions/s} \cdot \text{Ci}^{-1} \pm 300\%$ ). Calculation 6 computed the detector response to only the fission source to be  $3166 \text{ reactions/s} \cdot \text{Ci}^{-1} \pm 1.0\%$ . So, from these calculations it appears that the HEU threat object increased the HPGe detector response by only 3.2%—a very small effect. This is probably the best

way to simulate the change in detector response due to the presence of the nuclear material (ignoring the small amount of signal coming from the cargo material that the uranium displaced).

The speedup results (ratio of FOMs) for the other combinations of cargo material and specific detector are shown in Table III. For cargo containers without HEU, the CADIS calculations computed the same result as the analog calculation but with a much higher FOM (speedups in the range of 6 to 132). For the cases of cargo containers with HEU, the two-step CADIS method also calculated the same result as the analog method but with a much lower relative uncertainty for a given amount of calculation time (speedups in the range of 4 to 87).

Also shown in Table III is the change in detector response due to the presence of the HEU. The ratio of the response due to just the fission source (calculation 6) to the response from the source, the fission, and active background (calculation 5) is shown in the column titled “Fission/Total.” For the nine combinations examined in this study, the change in detector response due to the presence of nuclear material is small, from <11% to as low as 0.3%. The statistical uncertainties on the fission/total ratios were all <4% of the ratio value.

The spectral shapes of particles inside the detectors were also investigated. For the combinations in this study, the spectra of particles arriving at the detector from fission were shaped very similarly to the spectra coming from the surrounding materials. The spectra from the HPGe detector for the medium-density DHS iron/organic mixture are shown in Fig. 7 as an example. The neutron

TABLE III

Results Summary for Nine Combinations of Cargo Container Material and Detector

Material and Detector	Speedup		Fission/ Total (%)
	Without HEU	With HEU	
PNNL hydrogenous (0.2 g/cm <sup>3</sup> )			
Sodium iodide detector	10	16	4.7
HPGe detector	93	72	10.7
Helium-3 detectors	114	87	1.3
DHS iron/organic mixed cargo (0.4 g/cm <sup>3</sup> )			
Sodium iodide detector	6	4	2.8
HPGe detector	32	20	3.2
Helium-3 detectors	60	46	2.3
PNNL high-iron mixed cargo (0.6 g/cm <sup>3</sup> )			
Sodium iodide detector	21	14	0.8
HPGe detector	132	74	1.1
Helium-3 detectors	96	64	0.3

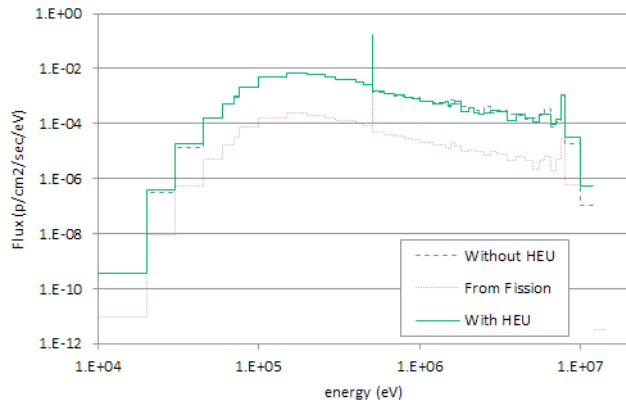


Fig. 7. Energy-dependent photon flux in the HPGe detector with HEU, without HEU, and only from HEU fission.

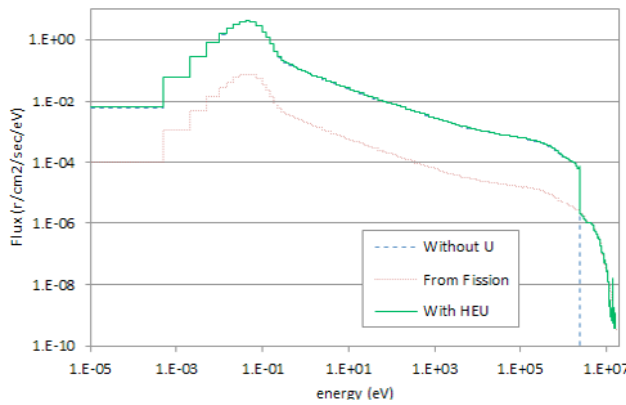


Fig. 8. Energy-dependent neutron flux in the <sup>3</sup>He detector with HEU, without HEU, and only from HEU fission.

spectra in the <sup>3</sup>He tubes were slightly different; a few neutrons above the source energy of 2.45 MeV were detected, but the number of neutrons in this range was very small compared with the rest of the spectra (shown in Fig. 8).

### III.C. Fishing Trawler

The third example problem in this study is an active interrogation system that uses a 20-MeV electron bremsstrahlung spectrum above 1 MeV, collimated into a beam with a total width of 1 deg. This source, emitting  $1 \times 10^{10}$  photons/s, is collocated with two neutron detectors (<sup>3</sup>He and a plastic scintillator) that are 25 m from the side of the boat. The standard threat object (a 25-kg sphere of HEU) is located in the main hold of the trawler, which is surrounded by a homogenous mixture representing fish and ice. The beam is pointed directly at the HEU sphere. The boat shown in Fig. 9 is a simplified model of a fishing trawler made up by the authors.

The multistep approach for this problem is more involved than for the previous problems. Here, the photon source can cause photofission in the HEU and can also cause the creation of photo-neutrons in the surrounding materials (deuterium in the fish/ice mixture and iron in the hull) via the giant dipole resonance effect.

The first step in the process used an FW-CADIS calculation to determine the photonuclear reaction rates as a function of space and energy in the HEU and surrounding materials. This was a photon-only calculation. The importance map for 10-MeV photons for this step is shown in Fig. 10, and the resulting reaction rate mesh tallies for the HEU, the fish/ice mixture in the hold, and the steel hull of the ship are shown in Figs. 11, 12, and 13, respectively. Figures 11, 12, and 13 show the photonuclear reaction rate in each material separately. Note that the HEU (Fig. 11) is at the center of the main hold (Fig. 12), which is in the center of the ship (Fig. 13). This calculation took 11 h (forward  $S_N$ , 2 h; adjoint  $S_N$ , 1 h; and Monte Carlo, 8 h).

The photonuclear reaction rates were then combined with neutron emission spectra to create neutron sources. These became the source in the second step, which determined the neutron-induced fission rate inside the HEU. This was a neutron-only calculation, and the final fission rate tally was converted into a neutron source for the third step. The computer time was 1 h for

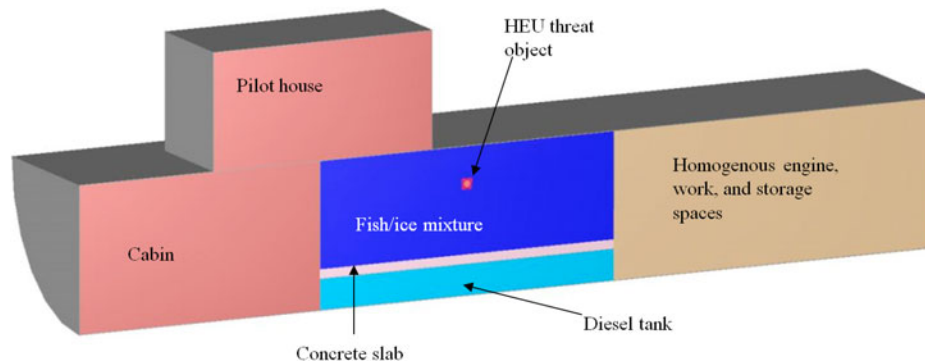


Fig. 9. Cutaway view of the simple model of a fishing trawler with HEU hidden in the main hold.

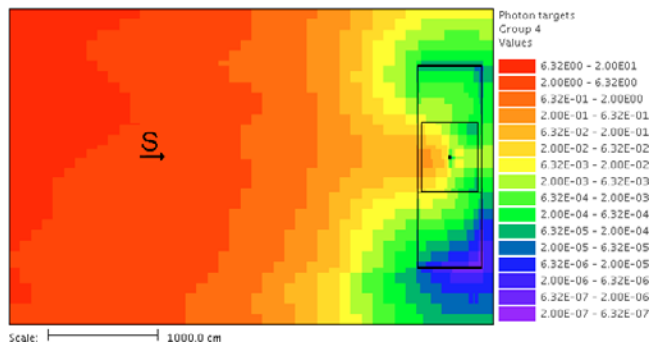


Fig. 10. Importance map target weight values for 10-MeV photons, shown with the source position (S) and the trawler (right) containing the HEU in the center of the main hold.

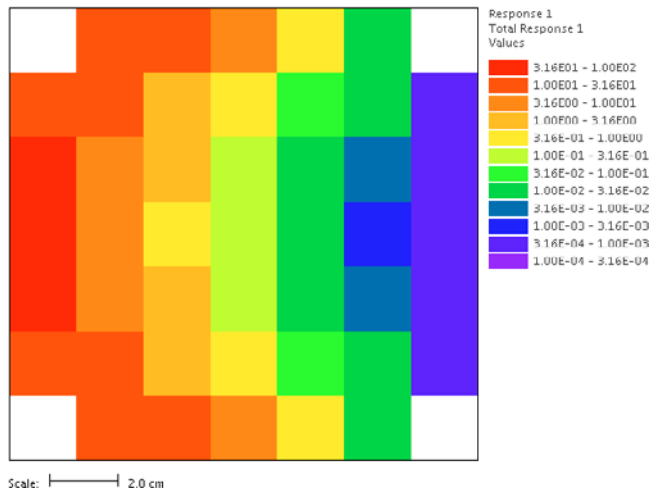


Fig. 11. Photonuclear reaction rate ( $s^{-1}/cm^3$ ) in the HEU.

the adjoint  $S_N$  calculation and 1 h for the Monte Carlo calculation.

The third step was to combine the photo-neutron sources from the HEU, the fish/ice mixture, and the hull, as well as the neutrons from the HEU neutron-induced fission, and compute the detector responses. This was also a neutron-only calculation and took 9.5 h (forward  $S_N$ , 0.75 h; adjoint  $S_N$ , 0.75 h; and Monte Carlo, 8 h). The importance map for neutron transport from the trawler to the detectors is shown in Fig. 14. The final results for the two detector responses from both the active background and the HEU sources are shown in Table IV. Also shown in Table IV are the detector responses from just the HEU fission sources (photofission computed in the first step and neutron-induced fission from the second step). Comparing these responses to the detector responses using all of the sources shows that the HEU accounted for less than one-millionth of the total detector count rates. Note

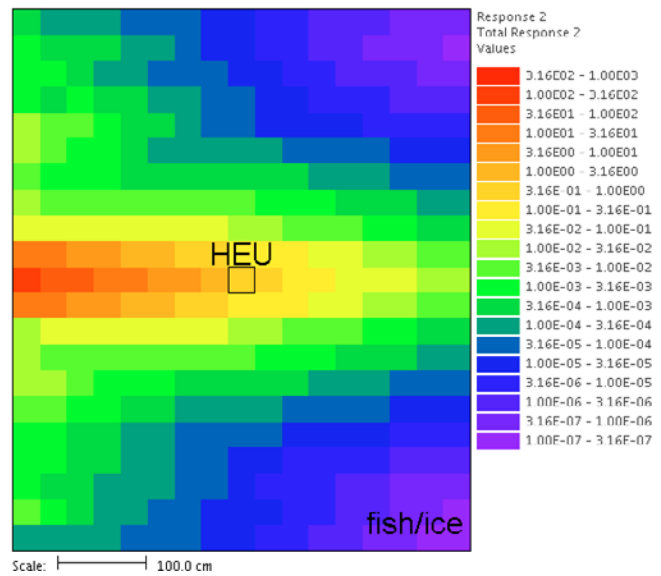


Fig. 12. Photonuclear reaction rate ( $s^{-1}/cm^3$ ) in the main hold containing a fish/ice mixture.

that Figs. 10 through 14 are all for the  $z$ -plane containing the threat object, all oriented the same way.

The final example problem contains two features that cannot be modeled in the public release of MAVRIC in SCALE 6.1: (a) the collimated beam cannot be modeled in a forward Denovo calculation (for FW-CADIS), and (b) SCALE 6.1 libraries currently do not include photonuclear cross-section data. To address the first issue, a special version of Denovo was used that could model anisotropic point sources. For the second issue, continuous-energy ENDF/B-VII photonuclear cross sections were taken from the MCNPX data Web site<sup>b</sup> and collapsed to the appropriate multigroup energy structure. These multigroup photonuclear cross sections were then entered into MAVRIC as response functions. A separate code was also written and used to convert energy-dependent photonuclear reaction rates into neutron sources using neutron emission spectra derived from MCNPX calculations. MCNPX was executed using its event generator mode to tally the neutrons produced by photonuclear interactions for the various materials in the trawler model (see the “noact=2” option on the LCA input card).

#### IV. SUMMARY AND FUTURE WORK

The three examples in this study demonstrate that the CADIS methodology can be applied in a multistep approach to active interrogation problems. This procedure allows variance reduction to be applied at each step in a

<sup>b</sup><https://mcnpx.lanl.gov/data.html>.

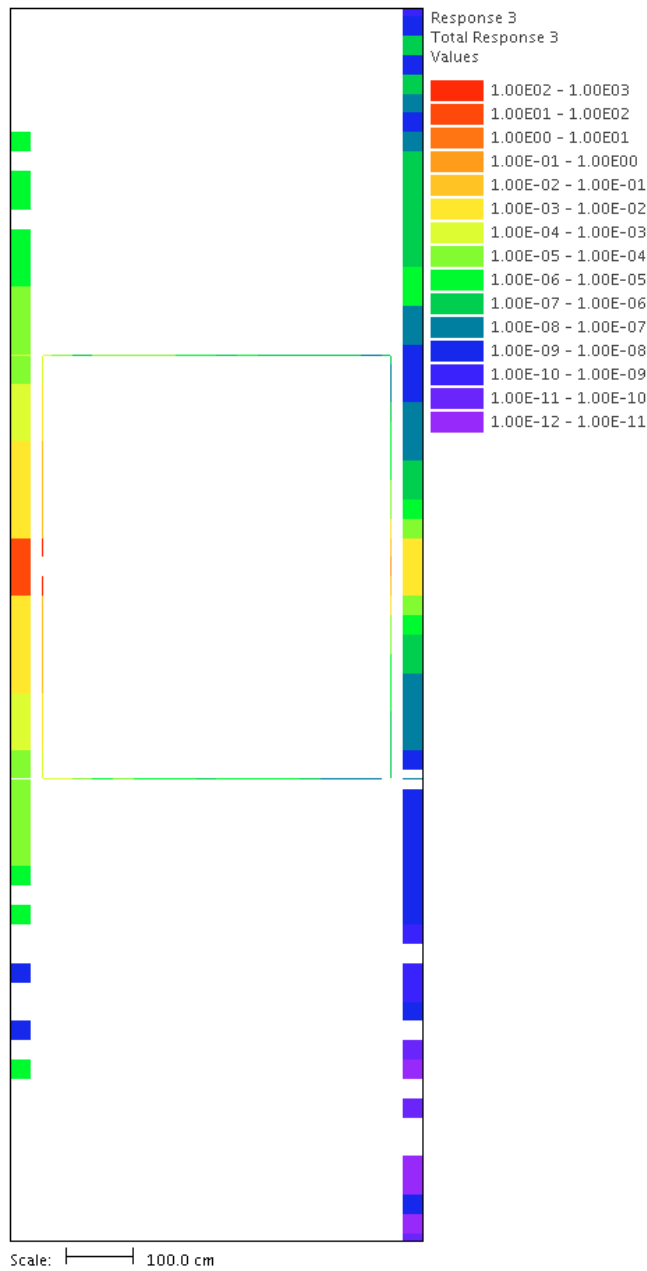


Fig. 13. Photonuclear reaction rate ( $s^{-1}/cm^3$ ) in the hull and steel materials.

straightforward manner to yield correct results more efficiently. When CADIS was used for the variance reduction, impressive gains in efficiency compared to analog calculations were seen. Since the problem was broken into several steps, some parts could easily be reused in similar problems, again saving time.

These example problems also illustrate the difficulties associated with detecting SNM using active interrogation systems. With improved simulation efficiency, parameter studies could be used to better characterize the

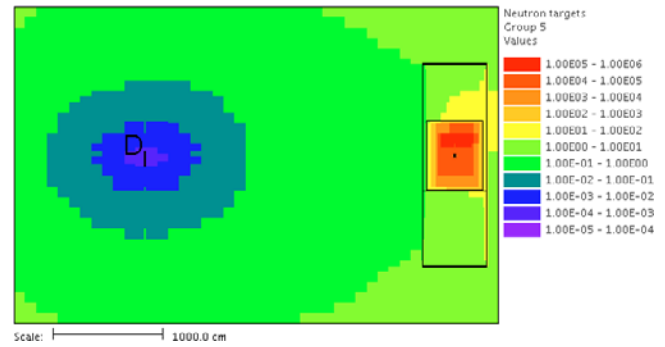


Fig. 14. Importance map target weight values for 1-MeV neutrons, shown with the detector panel (D) and the trawler (right) containing the HEU in the center of the main hold.

effectiveness of various proposed active interrogation systems with different sources, cargo materials, standoff geometries, detectors, etc.

As the results presented in this paper demonstrate the effectiveness of the hybrid methods for improving the efficiency of active interrogation problems, future work is recommended to further automate the analysis steps and hence simplify the use of these methods. First, hybrid codes such as MAVRIC could be modified to more easily facilitate generation of the multiple deterministic-based importance functions required for these analyses. Second, Monte Carlo codes such as Monaco could be modified to enable the use of multiple goal-based importance functions that depend on a particle's relevance to the ultimate goal of the simulation (e.g., particles originating from the active interrogation source are encouraged toward the threat object by one importance function, while particles emanating from the threat object are encouraged toward the detector with a different importance function). In such a system, it would be desirable for the user to be able to simply specify terms such as the interrogating source, the specific reactions to make induced sources, and the final detector area in a single input file. The code (e.g., MAVRIC) could then decompose the problem into separate steps that create the individual importance maps. Then, during the Monte Carlo simulation, after a given particle undergoes a specified reaction (e.g., fission in a threat object), it would switch importance maps for the progeny of the specified reaction. At each of the specified interactions, the primary particle could be split such that its transport could continue with each of the available importance maps, thereby allowing an accurate simulation of the detector response due to the presence of SNM and the active background. Enabling this process in a single Monte Carlo simulation would eliminate concerns and/or need for efforts related to ensuring that the statistical uncertainties in the calculated source for use in the second step of the multiple-step approach are adequately small. Further research on

TABLE IV  
 Detector Response Results for the Fishing Trawler

	All Neutron Sources		HEU Fission Only	
	Interactions (s <sup>-1</sup> )	Relative Uncertainty (%)	Interactions (s <sup>-1</sup> )	Relative Uncertainty (%)
Helium-3 ( <i>n, p</i> ) Plastic scintillator	1.44E+00 <sup>a</sup> 5.68E+02	5.5 3.5	2.95E-07 1.74E-04	14.0 8.1

<sup>a</sup>Read as 1.44 × 10<sup>0</sup>.

methods to normalize (or make consistent) the importance maps is also needed.

**ACKNOWLEDGMENT**

This work was sponsored by the Laboratory Directed Research and Development program at Oak Ridge National Laboratory.

**REFERENCES**

1. J. T. MIHALCZO, “Radiation Detection from Fission,” ORNL/TM-2004/234, Oak Ridge National Laboratory (Nov. 2004).
2. J. T. MIHALCZO, “Detection for Active Interrogation of HEU,” ORNL/TM-2004/302, Oak Ridge National Laboratory (Dec. 2004).
3. C. E. MOSS et al., “Comparison of Active Interrogation Techniques,” *2005 IEEE Nuclear Science Symposium Conference Record*, Puerto Rico, October 23–29, 2005, Vol. 1, p. 329, IEEE (2005).
4. D. E. PEPLow, “Monte Carlo Shielding Analysis Capabilities with MAVRIC,” *Nucl. Technol.*, **174**, 289 (2011).
5. “SCALE: A Modular Code System for Performing Standardized Computer Analyses for Licensing Evaluations,” ORNL/TM-2005/39, Version 6, Vols. I, II, and III, Oak Ridge National Laboratory (Jan. 2009).
6. J. C. WAGNER and A. HAGHIGHAT, “Automated Variance Reduction of Monte Carlo Shielding Calculations Using the Discrete Ordinates Adjoint Function,” *Nucl. Sci. Eng.*, **128**, 186 (1998).
7. A. HAGHIGHAT and J. C. WAGNER, “Monte Carlo Variance Reduction with Deterministic Importance Functions,” *Prog. Nucl. Energy*, **42**, 1, 25 (2003).
8. S. W. MOSHER et al., “Automated Weight-Window Generation for Threat Detection Applications Using ADVANTG,” *Proc. Int. Conf. Advances in Mathematics, Computational Methods, and Reactor Physics (M&C 2009)*, Saratoga Springs, New

York, May 3–7, 2009, American Nuclear Society (2009) (CD-ROM).

9. T. M. EVANS et al., “Denovo: A New Three-Dimensional Parallel Discrete Ordinates Code in SCALE,” *Nucl. Technol.*, **171**, 171 (2010).
10. D. E. PEPLow, S. W. MOSHER, and T. M. EVANS, “Hybrid Monte Carlo/Deterministic Methods for Streaming/Beam Problems,” presented at American Nuclear Society Joint Topl. Mtg. Radiation Protection and Shielding Division, Isotopes and Radiation Division, and Biology and Medicine Division, Las Vegas, Nevada, April 19–23, 2010.
11. J. C. WAGNER, E. D. BLAKEMAN, and D. E. PEPLow, “Forward-Weighted CADIS Method for Global Variance Reduction,” *Trans. Am. Nucl. Soc.*, **97**, 630 (2007).
12. D. E. PEPLow, E. D. BLAKEMAN, and J. C. WAGNER, “Advanced Variance Reduction Strategies for Optimizing Mesh Tallies in MAVRIC,” *Trans. Am. Nucl. Soc.*, **97**, 595 (2007).
13. D. E. PEPLow, T. M. EVANS, and J. C. WAGNER, “Simultaneous Optimization of Tallies in Difficult Shielding Problems,” *Nucl. Technol.*, **168**, 785 (2009).
14. X-5 MONTE CARLO TEAM, “MCNP—A General Monte Carlo N-Particle Transport Code, Version 5—Volume II: User’s Guide,” LA-CP-03-0245, Los Alamos National Laboratory (2008).
15. “MCNPX User’s Manual Version 2.7.0,” D. PELOWITZ, Ed., LA-CP-11-00438, Los Alamos National Laboratory (2011).
16. J. T. MIHALCZO et al., “Physical Description of Nuclear Materials Identification System (NMIS) Signatures,” *Nucl. Instrum. Methods Phys. Res., Sect. A*, **450**, 531 (2000).
17. J. T. MIHALCZO et al., “NMIS Plus Gamma Spectroscopy for Attributes of HEU, PU, and HE Detection,” *Nucl. Instr. Methods Phys. Res., Sect. B*, **213**, 378 (2004).
18. *IAEA Safeguards Glossary, 2001 Edition*, International Atomic Energy Agency (2002).
19. L. E. SMITH et al., “Viability Study for In-Transit Screening of Maritime Cargo: Final Report,” PNNL-17780, Pacific Northwest National Laboratory (Aug. 2008).